Tunable protein harmonic diffractive micro-optical elements

Yun-Lu Sun,[1] Dong-Xu Liu,[1] Wen-Fei Dong,[1,3] Qi-Dai Chen,[1] and Hong-Bo Sun[1,2,4]

[1]*State Key Laboratory on Integrated Optoelectronics, College of Electronic Science and Engineering, Jilin University, 2699 Qianjin Street, Changchun 130012, China*

[2]*College of Physics, Jilin University, 119 Jiefang Road, Changchun 130023, China*

[3]*e-mail: dongwf@jlu.edu.cn*

[4]*e-mail: hbsun@jlu.edu.cn*

Received April 2, 2012; revised May 20, 2012; accepted May 21, 2012; posted May 22, 2012 (Doc. ID 165899); published July 13, 2012

Herein, tunable protein harmonic diffractive microlenses (PHDMs) have been constructed by femtosecond laser direct writing from bovine serum albumin. With excellent three-dimensional topography, PHDMs show distinct harmonic diffractive features, such as similarly good imaging performance with smaller thickness than refractive lenses and well controlled minus chromatic dispersion compared with simple diffractive lenses (~5% focal length shift against ~21% of the protein Fresnel zone plate with the same radius under light with wavelength 450–659 nm). Owing to the nature of protein molecules as "building blocks," the focal length of the PHDM can be facilely tuned within seconds by changing the pH value (focal length tunability of up to ~20%).

OCIS codes: 170.0170, 160.1435, 000.1430.

The harmonic diffractive microlens (HDM) is an imaging element for which the length of the optical path between adjacent facets is an integer multiple p of the designed wavelength λ_0 [Fig. 1(a)] [1]. Compared with refractive lenses, HDMs have a smaller thickness for achieving similar imaging and focusing performance. More importantly, HDMs exhibit hybrid optical properties of both refractive and diffractive lenses because they have a common focus for a number of discrete wavelengths across the visible spectrum. This unique feature can highly suppress the diffractive element's chromatic dispersion compared with a modulo 2π phase-shift diffractive lens. Therefore, it has been widely applied in optical system design and integration [2]. However, for classical HDMs made of glass, quartz, polymer, etc., the lack of environmental responsiveness will limit their further applications. Compared with other tunable miniaturized refractive or diffractive lenses, such as liquid-based focus-tunable microlenses [3], tunable Fresnel diffractive lenses using nanoscale polymer-dispersed liquid crystals [4], hydrogel microparticles as dynamically tunable microlenses [5], etc., few reports have focused on the tunable HDMs, as far as we know. Therefore, in this Letter, we report the construction of protein-hydrogel-based continuous-relief harmonic diffractive microlenses (PHDMs), using a femtosecond laser direct writing (FsLDW) approach. With the help of excellent three-dimensional (3D) topography quality provided by FsLDW [6,7], distinct harmonic diffractive optical properties (well-controlled minus chromatic dispersion) and fine focusing and imaging performance are achieved here. Especially, PHDMs are endowed with unique pH-responsive behavior and good biocompatibility due to the nature of protein molecules used as "building blocks" [7].

Herein, the PHDM was designed as the schematic diagram of Fig. 1(a), where h was designed to be 3.3 μm and the radius was 30 μm. Commercial bovine serum albumin (BSA; 300–500 mg/mL in aqueous solution) was used as the building material for the FsLDW of 3D protein optical microdevices, with the assistance of methylene blue (MB; 0.6 mg/mL). In the case of methylene blue as a photosensitizer, the laser energy by two photon absorption is transferred to ground state oxygen to form a reactive oxygen species such as singlet oxygen ($^1O_2$) [8–10]. The singlet oxygen ($^1O_2$) can facilely catalyze the inter- or intramolecular covalent crosslinking of oxidizable protein residues (Tyr, Trp, His, Met, Cys, etc.), resulting in the formation of 3D protein microhydrogel [8–10]. By an oil-immersion objective with high-numerical aperture (60×, NA = 1.35), the beam from the femtosecond laser (80 MHz repetition rate,120 fs pulse width, 780 nm central wavelength) was focused in BSA aqueous solution tightly for proper optical density to induce the crosslinking of protein molecules in the central area of the focal spot. Then, protein microdevices were directly "written" out on a glass chip by computer-programmed 3D scanning of the focused laser spot in BSA aqueous solution. Here, the vertical and horizontal scanning movements of the focused spot were achieved simultaneously by the piezo stage and the two-galvano-mirror set [11,12]. After FsLDW, the sample was rinsed

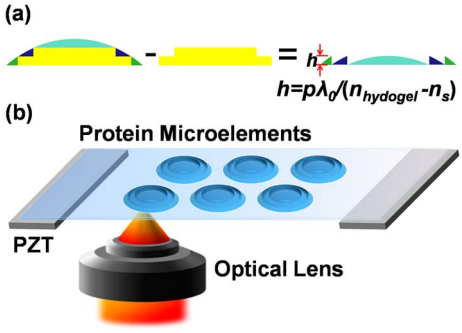

Fig. 1. (Color online) (a) Schematic diagram of the design of continuous-relief harmonic diffractive microlens. $\lambda_0 = 550$ nm, $p = 3$. The element's thickness is h (3.3 μm). n_s (1.0 for air) is the refractive index of the surrounding, and $n_{hydrogel}$ (~1.50) is the refractive index of the protein hydrogel; (b) experimental schematic for FsLDW of protein microelements.

in water to remove unreacted protein. Then as-formed protein microstructures were left on the chip [Fig. 1(b)].

As is well known, the topography (3D shape and surface roughness) plays important roles in imaging performances of protein micro-optics. Thus, precise control of surface quality and 3D accuracy was the prerequisite in this work [7,13,14]. Herein, a stable FsLDW system was built up and equipped with an output feedback system and proper enclosure. Meanwhile, numerous optimized parameters—for instance, of appropriate laser power (~15 mW, measured before the objective lens), exposure time (1000 μs at every point), and scanning step (100 nm in three dimensions)—were utilized during FsDLW processing. As a result, PHDMs with higher surface smoothness and improved mechanical strength were facilely fabricated. In Fig. 2, the micro-optics were investigated and characterized by optical microscopy, scanning electron microscopy (SEM), and atomic force microscopy (AFM) (Fig. 2). The average surface roughness (Ra) in air was ~10 nm, measured by AFM, which was low enough for achieving good optical performance [Figs. 2(b) and 2(e)]. In addition, though it was designed to be 3.3 μm, the actual height of the PHDMs dried in air was only ~2 μm [Fig. 2(e)]. AFM results showed that there was no structural disruption caused by a fabricating error, and no disconnected area was observed at the bottom phase-discontinuous points marked in Fig. 2(e). Therefore, the height loss was caused mainly by dehydration of protein hydrogel in air.

Owing to the fine topography, the protein relief microlens exhibited excellent optical performances in phosphate buffered saline buffer (pH = 7.0) (Fig. 3). Figure 3(b) displays the normalized light intensity distribution along the dotted line across the center of the PHDM in Fig. 3(a). The full width at half maximum (FWHM) of the curve was ~9 μm (for a PHDM with a radius of 30 μm and a height of 3 μm). However, in our previous work, a protein spherical microlens with a radius of 20 μm and a height of 5 μm exhibited an FWHM of ~15 μm. Obviously, the difference indicated that the lens efficiency of a protein continuous-relief microlens was higher compared with a refractive microlens [7]. Contrary to usual refractive lenses, a minus chromatic dispersion was found in as-formed PHDMs. Fig. 3(c) would be useful for optical system design—for example, the achromatization of lens systems. Figure 3(d) shows the focal lengths of PHDMs for monochromatic light with different wavelengths and white light in air. It was tested that the largest focal length shift was ~5%, much smaller than the value of ~21% for a protein Fresnel zone plate made also by FsLDW with the same radius as a control. This result demonstrated that the chromatic aberration was strongly reduced, compared with simple diffractive optical elements. Thus, the imaging ability of PHDMs was found to be as good as that of protein refractive microlenses [Fig. 3(e)] [7].

Besides these optical properties, PHDMs also exhibited more interesting and valuable features, including biocompatibility and stimuli-responsive tunability. As shown in Fig. 4, when immersed into either a high pH or a low pH buffer, the PHDM started to swell. And it could shrink back to the original size and shape after changing the pH value. The swelling or shrinking profiles happen rapidly (within seconds) when solvent diffuses into the protein-hydrogel network and induces the strong electrostatic repulsion between charged weak acid and base pendant groups. It is the microminiaturization of protein microdevices that helps to obtain the high response speed because the diffusion time of solvent molecules scales with the diffusion length (L) of polymer as L^2 [7,15]. Because the extent of PHDM expansion in the horizontal direction was highly restricted by a glass surface, the expansion along the lateral direction became much more pronounced. The thickness of the relief lens swelled to about 150% (from ~3 to ~5 μm) when the pH

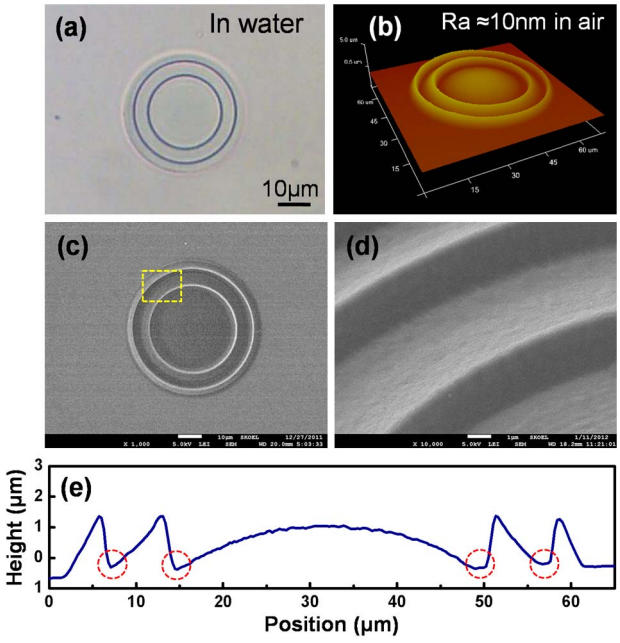

Fig. 2. (Color online) (a) Optical microscopy picture of a PHDM in water; (b) atomic force microscopy (AFM) image of the PHDM in (a). Roughness average (Ra) is ~10 nm; (c) scanning electron microscopy image of the PHDM in (a). (d) Enlarged view of the marked area in (c), 30 deg tilted; (e) curve of section contour of the PHDM in (a) characterized by AFM image in air.

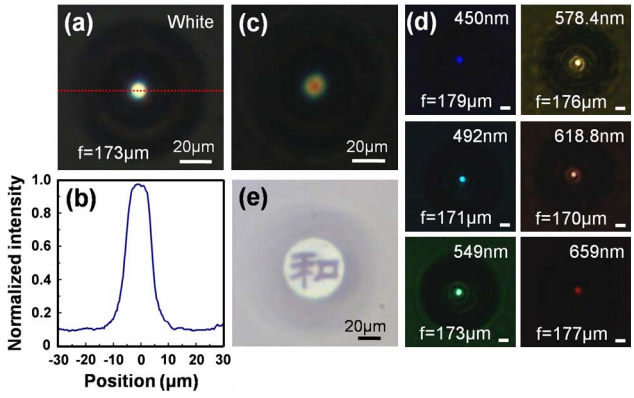

Fig. 3. (Color online) (a) Focusing test of a PHDM in air; (b) normalized light intensity distribution along the dotted line across the center of (a). (c) Minus chromatic dispersion property of the PHDM in air; (d) focal lengths of the PHDM for monochromatic light with different wavelengths in air. Scale bar, 10 μm. (e) Focused image of the PHDM.

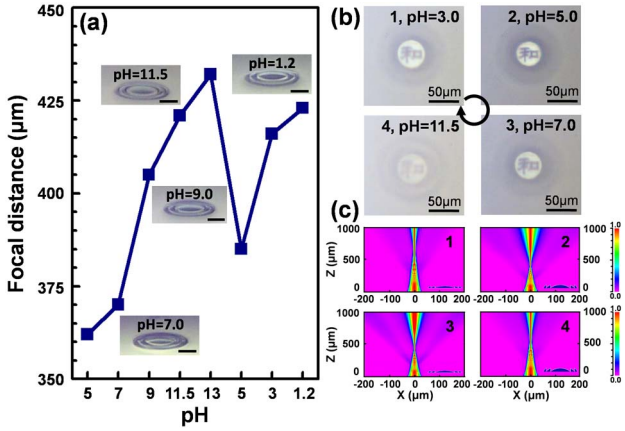

Fig. 4. (Color online) (a) Focal lengths of the PHDM in buffers vs. pH value. Inset: SEM images of side view of the PHDM under different pH. Scale bar, 20 μm; (b) reversible imaging adjustment by pH changing from 3.0 to 11.5; (c) soft simulation of pH-responsive focal lengths.

value was changed from 5.0 to 13.0 or 1.2, as demonstrated by the insets of Fig. 4(a). Meanwhile, PHDMs still held fine topography during pH processing, as shown in the insets of Fig. 4(a), which was essential for their imaging and focusing features during tuning [Fig. 4(b)]. When the pH value was increasing from 3.0 to 11.5, the image became clear at first and then out of focus step by step [Fig. 4(b), 1–4]. It was observed that the focal length became larger when pH value increased from 5.0 to 13, and decreased from 5.0 to 1.2 [Fig. 4(a)]. During the pH treatment, it was proved that the PHDMs could tolerate strong acids (pH = 1.2) or alkalis (pH = 13.0), without any damage of their optical performance.

The 3D shape (mainly the thickness here, h) and the refractive index of protein hydrogel ($n_{hydrogel}$) were the two main factors determining the adjustable imaging and focusing properties of the PHDMs. In this work, the tunable focal length can be simulated by Rsoft. The refractive index of buffer (n_{buffer}) with a different pH value was almost constant (~1.33), as proven by Abbe refractometer measurement. If $n_{hydrogel}$ was fixed at 1.45 (the estimated value in our previous work [7]) and $n_s = n_{buffer} = 1.33$, the simulated focal length (f_{sim}) decreased from ~550 to ~400 μm with the thickness of the PHDM increasing from 3 to 6 μm (the largest expansion possible for protein hydrogel [15]), as shown in Fig. 4(c), 1 and 2. However, these simulations did not agree with the experimental results. In fact, f increased from ~360 to ~435 μm when the PHDMs swelled with pH changing from 5.0 to 13.0 or 1.2 [Fig 4(a)]. The difference means that $n_{hydrogel}$ does not keep constant during pH treatment, and its changes should be taken into consideration. In our previous work, we found that $n_{hydrogel}$ decreased from ~1.50 to ~1.40 after swelling [7]. So, at pH = 5.0 ($n_s = n_{buffer} = 1.33$, $n_{hydrogel} = 1.53$, and $h = 3$ μm), f_{sim} was calculated to be ~360 μm [Fig. 4(c), 3], based on Rsoft simulation. And at pH 13.0 ($n_s = n_{buffer} = 1.33$, $n_{hydrogel} = 1.41$, $h = 6$ μm), f_{sim} increased to ~440 μm [Fig. 4(c), 4]. Obviously, these simulated results coincided with the experiment, which indicated that $n_{hydrogel}$ played a more important role on f of PHDMs. Thus, when the pH value changes from neutral to basic or acid, PHDMs start to swell, which will result in a decrease of $n_{hydrogel}$ and an increase of f.

In summary, we have reported a tunable protein harmonic diffractive 3D continuous-relief microlens constructed by femtosecond laser direct writing from BSA. By careful control of surface quality and 3D accuracy, PHDMs have distinct harmonic diffractive features—for instance, of similarly good imaging performance with smaller thickness and well-controlled minus chromatic dispersion. Owing to the nature of protein molecules as building blocks, PHDMs exhibit unique dynamic tunability of imaging and focusing properties (high focal length tunability of up to ~20%), which shows great promise for optical and biomedical applications. The devices reported on in this Letter, combined with recent reported novel protein-based micro/nanodevices, such as protein microwaveguides [16] and protein two-dimensional photonic crystal [17,18], may enable a new concept of protein-based photonics to revolutionize the new generation of polymeric and organic-based optical microdevices.

This work was supported by the National Science Foundation of China (grants 61137001, 90923037, 61077066, and 91123029).

References

1. D. W. Sweeney and G. E. Sommargren, Appl. Opt. **34**, 2469 (1995).
2. T. Ammer, M. T. Gale, and M. Rossi, Opt. Eng. **41**, 3141 (2002).
3. L. Dong, A. K. Agarwal, D. J. Beebe, and H. Jiang, Nature **442**, 551 (2006).
4. H. W. Ren, Y. H. Fan, and S. T. Wu, Appl. Phys. Lett. **83**, 1515 (2003).
5. J. Kim, M. J. Serpe, and L. A. Lyon, J. Am. Chem. Soc. **126**, 9512 (2004).
6. T. Hessler, M. Rossi, R. E. Kunz, and M. T. Gale, Appl. Opt. **37**, 4069 (1998).
7. Y. L. Sun, W. F. Dong, R. Z. Yang, X. Meng, L. Zhang, Q. D. Chen, and H. B. Sun, Angew. Chem. Int. Ed. **51**, 1558 (2012).
8. J. D. Spikes, H. R. Shen, P. Kopeckova, and J. Kopecek, Photochem. Photobiol. **70**, 130 (1999).
9. M. J. Davies, Photochem Photobiolog. Sci. **3**, 17 (2004).
10. H. R. Shen, J. D. Spikes, C. J. Smith, and J. Kopecek, J Photochem. Photobiol. A: Chem. **130**, 1 (2000).
11. Q. D. Chen, D. Wu, L. G. Niu, J. Wang, X. F. Lin, H. Xia, and H. B. Sun, Appl. Phys. Lett. **91**, 171105 (2007).
12. D. Wu, L. G. Niu, Q. D. Chen, R. Wang, and H. B. Sun, Opt. Lett. **33**, 2913 (2008).
13. D. Wu, S. Z. Wu, L. G. Niu, Q. D. Chen, R. Wang, J. F. Song, H. H. Fang, and H. B. Sun, Appl. Phys. Lett. **97**, 031109 (2010).
14. K. Takada, H. B. Sun, and S. Kawata, Appl. Phys. Lett. **86**, 071122 (2005).
15. B. Kaehr and J. B. Shear, PNAS **105**, 8850 (2008).
16. S. T. Parker, P. Domachuk, J. Amsden, J. Bressner, J. A. Lewis, D. L. Kaplan, and F. G. Omenetto, Adv. Mater. **21**, 2411 (2009).
17. J. J. Amsden, P. Domachuk, A. Gopinath, R. D. White, L. D. Negro, D. L. Kaplan, and F. G. Omenetto, Adv. Mater. **22**, 1746 (2010).
18. J. P. Mondia, J. J. Amsden, D. Lin, L. D. Negro, D. L. Kaplan, and F. G. Omenetto, Adv. Mater. **22**, 4596 (2010).